peptide chain from one tRNA molecule to the other. It is not at all clear how this is accomplished, although it has been suggested that the two codons become unstacked during the reading process so that in effect the messenger "turns a corner" while it is read.[28] This remains an exciting area for further research work.

Important work by Erdmann and his colleagues[29] has suggested that the T-ψ-C loop may become disengaged from the D loop inside the ribosome so that it can then hydrogen bond with the 5S RNA of the ribosome. This interaction may be an important component in the translocation of tRNA from aminoacyl site to the peptidyl site. If this is true, the tRNA molecule undergoes a conformational change within the ribosome. Determination of the nature of these events remains an important research goal. It is possible that this conformational change is triggered by codon–anticodon interactions, and this may be a consequence of the fact that the tRNA molecule as a whole exhibits long-range order.[4] Thus interactions at one end may give rise to a change in reactivity or in conformation at a more remote part of the molecule.

The end product of biological crystallography is the determination of three-dimensional structure. However, the major problem to be solved is that of understanding biological function. In this regard, structural information is particularly valuable in generating reasonable models which can be explored to explain aspects of function. In tRNA research we now have a firm view of the three-dimensional structure of the molecule. What remains to be understood is how this three-dimensional structure is used to carry out the various functions of tRNA in biological systems.

Elucidation of the structure of tRNA involved the work of many colleagues as cited in the bibliography, and I wish to acknowledge the important role which they played in this effort. I thank especially S. H. Kim, G. Quigley, and F. L. Suddath, who worked for many years on this project. Research for this work was supported by grants from the National Institutes of Health, National Science Foundation, National Aeronautics and Space Administration, and the American Cancer Society.

(28) A. Rich in "Ribosomes", M. Nomura, A. Tissières, and P. Lengyel, Ed., Cold Spring Harbor Laboratory, New York, N.Y., 1974, p 171.
(29) V. A. Erdmann, M. Sprinzl, and O. Pongs, *Biochem. Biophys. Res. Commun.*, **54**, 942 (1973); D. Richter, V. A. Erdmann, and M. Sprinzl, *Proc. Natl. Acad. Sci. U.S.A.*, **71**, 3326 (1974).

Application of High-Resolution Nuclear Magnetic Resonance Spectroscopy in the Study of Base Pairing and the Solution Structure of Transfer RNA

Brian R. Reid* and Ralph E. Hurd

Biochemistry Department, University of California, Riverside, California 92521

Received February 17, 1977

The functional aspects of tRNA and its structure as revealed by x-ray crystallography have already been described in this issue and elsewhere.[1-3] The crystallographic approach yields a static structure of tRNA in the crystalline solid state with unrivaled precision. However, the molecule functions biologically in the liquid state, and it is important to ask if the solution conformation (or conformations) is related to the crystal structure and whether there are important dynamic conformational equilibria in the solution structure. We have addressed ourselves to these questions using high-resolution nuclear magnetic resonance (NMR) as a spectroscopic probe of the structure of tRNA in solution.

Although there are several classes of protons in the various regions of the magnetic resonance spectrum of nucleic acids, perhaps the most informative spectral window is the extreme low-field region between −11 and −15 ppm downfield from the standard DSS (2,2-dimethylsilapentane-5-sulfonate) reference. We shall refer to this region as the low-field spectrum. Early NMR studies on model nucleosides in aprotic solvents by Katz and Penman[4] revealed that the ring NH protons of guanosine (N1H) and uridine (N3H) are highly deshielded and move even further downfield in the low-field spectrum upon forming hydrogen-bonded base pairs with their complementary nucleosides.

Although the ring NH protons of free monomers are rapidly exchangeable with water (and thus time-average into the large H_2O peaks at −4.65 ppm in aqueous solvents), in polymers such as tRNA the base–base hydrogen bonds have long lifetimes (seconds) in the interior of the water-inaccessible helices.[5]

These considerations led Kearns and Shulman and their collaborators to attempt the first low-field NMR

Brian R. Reid received his B.A. degree from Cambridge University and his Ph.D. from the University of California, Berkeley. He then held a Jane Coffin Childs postdoctoral fellowship at Dartmouth Medical School and in 1966 joined the Biochemistry Department at the University of California, Riverside, where he is Professor of Biochemistry. His research interests include structural studies on transfer RNA and aminoacyl-tRNA synthetase enzymes using a variety of physical methods, and the mechanism of protein–nucleic acid recognition.

Ralph E. Hurd received his B.A. degree from California State College, San Bernardino, in 1973. He is currently carrying out doctoral thesis research in the Biochemistry Department, University of California, Riverside, on the solution structure and conformational dynamics of regulatory and nonregulatory mutant tRNAs.

(1) S. H. Kim, F. L. Suddath, G. J. Quigley, A. McPherson, J. L. Sussman, A. H. J. Wang, N. C. Seeman, and A. Rich, *Science*, **185**, 435 (1974).
(2) J. D. Robertus, J. E. Ladner, J. T. Finch, D. Rhodes, R. S. Brown, B. F. C. Clark, and A. Klug, *Nature (London)*, **250**, 546 (1974).
(3) J. L. Sussman and S. H. Kim, *Science*, **192**, 853 (1976).
(4) L. Katz and S. Penman, *J. Mol. Biol.*, **15**, 220 (1966).
(5) S. W. Englander and J. J. Englander, *Proc. Natl. Acad. Sci. U.S.A.*, **53**, 370 (1965).

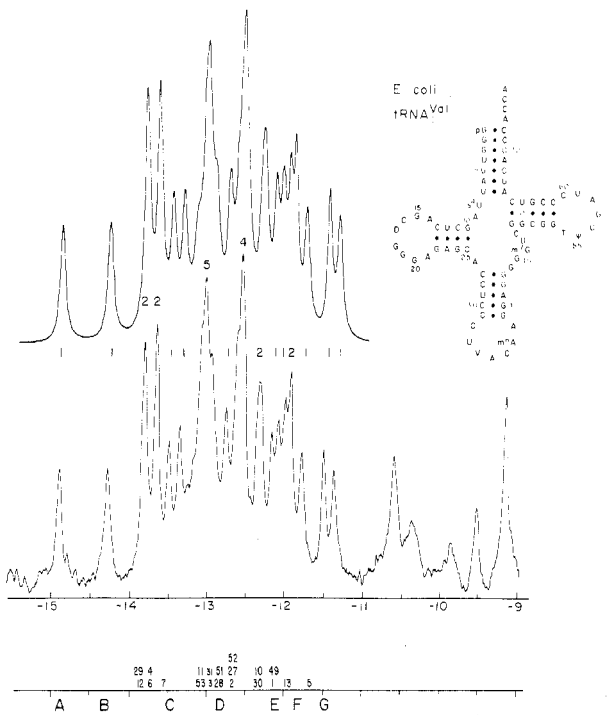

Figure 1. The low-field 360-MHz NMR spectrum of *E. coli* $tRNA^{Val}_1$ at 39 °C in the presence of excess magnesium. The lower trace is the experimental spectrum and the upper trace is a computer simulation. The tRNA concentration is 1 mM and the solvent is 10 mM sodium cacodylate, 100 mM NaCl, 15 mM $MgCl_2$, pH 7.0. The bottom line indicates the predicted secondary resonances and the extra tertiary resonances.

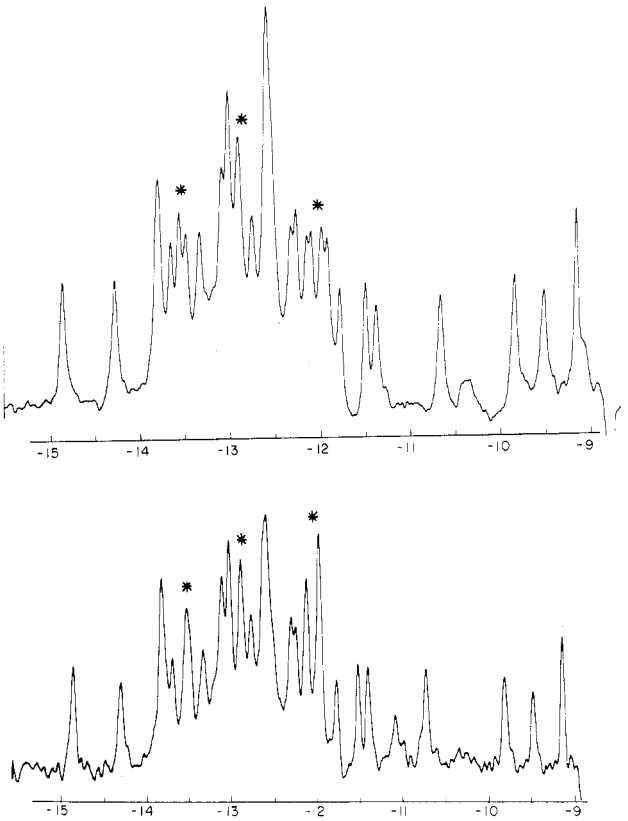

Figure 2. The low-field 360-MHz NMR spectrum of *E. coli* $tRNA^{Val}_1$ under minimal magnesium (upper) and no magnesium (lower) conditions at 35 °C. The tRNA concentration is 1 mM; the no-magnesium solvent contains 10 mM sodium cacodylate, 10 mM EDTA, pH 7.0, and the minimal magnesium spectrum is the same sample supplemented by 2-μL additions of magnesium chloride to a final concentration of approximately 8.8 mM magnesium. The resonances which shift with respect to the excess magnesium spectrum in Figure 1 are indicated with asterisks.

spectroscopic studies of tRNA in H_2O solvents some 5 to 6 years ago.[6-9] These studies indeed revealed a series of partially resolved resonances, and it became apparent that the low-field NMR spectrum monitors a single natural reporter group from each base pair (only one ring NH hydrogen bond) provided that the base-pair helical lifetime is ~10 ms or longer. The resolution observed among the low-field resonances from different base pairs is primarily due to the different nearest-neighbor environment in which a given G·C or A·U base pair is situated, i.e., the spectrum is sequence dependent. This sequence effect is caused by local induced magnetic fields resulting from the flow of electrons in the rings of neighboring bases (ring current shifts); the strength of these ring currents, and of the induced magnetic field, is different for the four nucleotides commonly found in RNA.

Hence, although the hydrogen-bonded ring NH of all G·C pairs must be considered to have the same unshifted inherent resonance position, each particular low-field G·C resonance will be differentially upfield shifted by values which depend on the identity and position of the four nucleotides in the two nearest neighbor base pairs (the inverse third-power distance dependence of this process results in next-to-nearest neighbors being less important but nevertheless significant). The A·U ring NH resonance, although at lower field, also exhibits a sequence-dependent chemical shift in RNA.

The initial problems to be addressed by tRNA low-field NMR spectroscopy are the number of low-field resonances (base pairs) and the assignment of the resolved peaks. The controversial point of the total intensity of intact tRNA low-field NMR spectra and the assignment of these spectra based on empirical ring-current shifts has been reviewed in this journal by Kearns and Shulman.[10] Previously tRNA spectra have been obtained by continuous wave (CW) spectroscopy using 1–4 h of signal-averaging on 1 mM tRNA samples. The spectra we shall show here were obtained on 5–6 mg of tRNA in 0.18 mL of buffer using correlation spectroscopy[11] with 10–15 min of signal-averaging.

How Many Base Pairs in tRNA in Solution?

Figure 1 shows the 360-MHz low-field correlation spectrum of *E. coli* $tRNA^{Val}_1$ (1 mM) in the presence of excess magnesium ion (15 mM) at 39 °C (lower spectrum). Between −11 and −15 ppm there are 17 peaks of unequal intensity. The peaks at −14.9, −14.3, −11.5, and −11.35 ppm are of equal intensity and correspond to a single proton. The integrated area is indicated at the top of each peak. The spectrum contains 27 low-field resonances, indicating the presence of 27 long-lived base pairs in solution. The value is

(6) D. R. Kearns, D. Patel, and R. G. Shulman, *Nature (London)*, **229**, 338 (1971).
(7) D. R. Kearns, D. Patel, R. G. Shulman, and T. Yamane, *J. Mol. Biol.*, **61**, 265 (1971).
(8) Y. P. Wong, D. R. Kearns, B. R. Reid, and R. G. Shulman, *J. Mol. Biol.*, **72**, 725 (1972).
(9) D. R. Kearns, D. R. Lightfoot, K. L. Wong, Y. P. Wong, B. R. Reid, L. Cary, and R. G. Shulman, *Ann. N.Y. Acad. Sci.*, **222**, 324 (1973).
(10) D. R. Kearns and R. G. Shulman, *Acc. Chem. Res.*, **7**, 33 (1974).
(11) J. Dadok and R. F. Sprecher, *J. Magn. Resonance*, **13**, 243 (1974).

corroborated by the computer-simulated spectrum above the experimental spectrum. In the computer simulation a series of Lorentzian lines of unit intensity having the experimental line width were adjusted horizontally until the experimental spectrum was duplicated. The simulation shown required 27 lines.

The spectrum of the same tRNA in the complete absence of magnesium (lower spectrum) and in "magnesium-starvation" conditions (upper spectrum) is shown in Figure 2. Between −11 and −15 ppm the former spectrum shows 19 peaks and the latter spectrum shows 21 peaks. Integration and computer simulation both indicate the presence of 27 low-field resonances in the spectrum and demonstrate that no base pairs are lost under these conditions. The low-field NMR spectrum of *E. coli* $tRNA^{Val}_1$ in the absence of magnesium at 35 °C has been claimed by Kearns and co-workers[12-14] to contain only 20 resonances. However, their spectra are poorly resolved which necessitated alternative, less-accurate, integration methods.[15]

Although no base pairs are lost at physiological temperature in the absence of magnesium, the spectra do reveal some interesting structural rearrangements detected by shifting of resonances. These magnesium-induced shifts (shown by asterisks) are very useful diagnostic clues to the tertiary structure in solution and will be discussed later. Since each base-pair resonance is sensitive to local ring-current shifts (which decrease with the third power of distance) from 3.4-Å stacked neighbors, it follows that easily detected shifts can result from local movement of as little as 0.5 Å or less.

We have carried out comparative low-field NMR studies on several other class 1 D4V5 tRNA species (these species contain four base pairs in their h_2U helix and a five-nucleotide variable loop containing m^7G). The correlation spectra of *E. coli* $tRNA^{Met}_m$ and *E. coli* $tRNA^{Gly}_3$ are shown in Figure 3. Figure 4 shows the correlation spectra of *E. coli* $tRNA^{His}$ and *E. coli* $tRNA^{Arg}_1$. In all cases the low-field integration and the computer simulation reveal the presence of the expected 20 secondary base-pair resonances plus an additional six or seven resonances.

We have extended these comparative studies to include 14 different class-1 tRNA species from *E. coli* and yeast; in each case the −11 to −15 ppm spectrum reveals 7 ± 1 extra resonances over and above those expected from the cloverleaf secondary structure. The tRNA species in this series are all structurally related to yeast $tRNA^{Phe}$, which is the only tRNA for which a three-dimensional crystal structure is available.[1-3] In the crystal structure there are several tertiary base-pairing interactions which involve extension of the h_2U helix and interaction of this extended helix with the rT loop; the tertiary interactions involving ring NH hydrogen bonds are U8–A14, G15–C48, G19–C56, m^7G46–G22, T54–A58, G26–A44, and possibly G18–ψ55.[3] We conclude that these crystallographic tertiary base pairs are responsible for the 7 ± 1 extra low-field resonances which we observe in the solution structure of yeast $tRNA^{Phe}$ and 13 other related class-1 tRNAs we have studied. Previous attempts to integrate poorly resolved

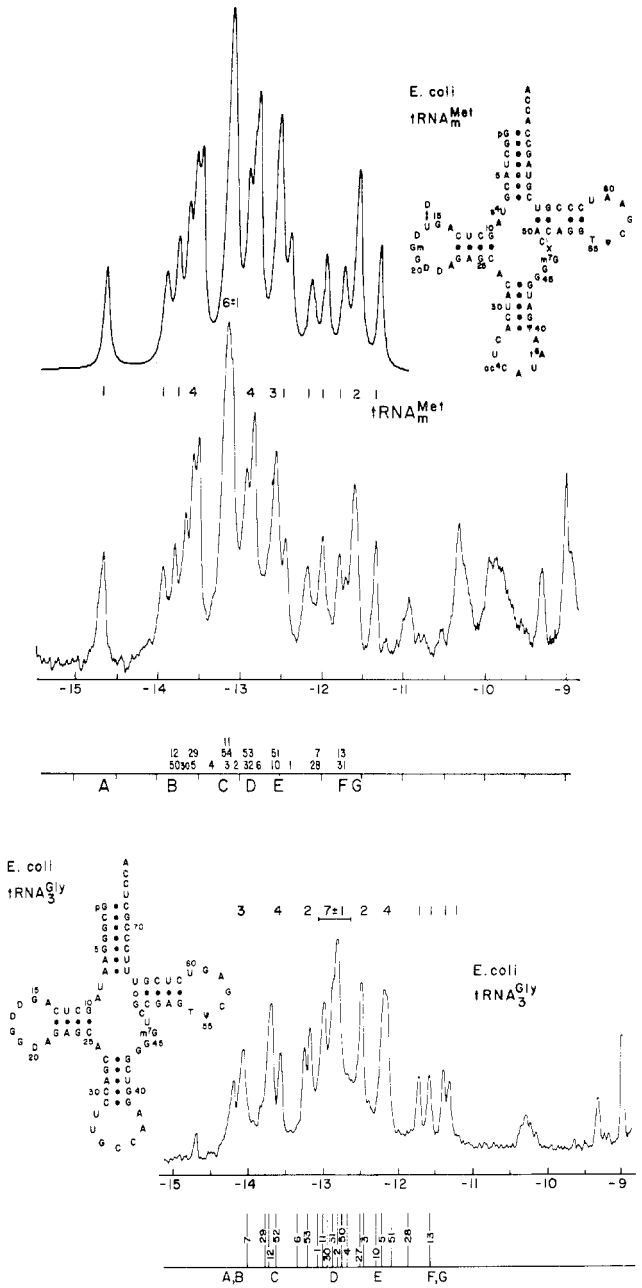

Figure 3. The low-field 360-MHz NMR spectra of *E. coli* $tRNA^{Met}_m$ and $tRNA^{Gly}_3$. Conditions are as in Figure 1. The predicted secondary resonances and extra tertiary resonances are shown at the bottom of each spectrum. The computer simulation of the $tRNA^{Met}_m$ spectrum is shown at the top.

class-1 tRNA low-field spectra claimed only −1 to +2 extra resonances attributable to tertiary structure.[10,12-14,16-21]

Identification and Assignment of Tertiary Resonances

The assignment of tertiary resonances is a relatively difficult task since the covalent cleavage and denatu-

(12) P. H. Bolton and D. R. Kearns, *Nature (London)*, **262**, 423 (1976).
(13) P. H. Bolton, C. R. Jones, D. Bastedo-Lerner, K. L. Wong, and D. R. Kearns, *Biochemistry*, **15**, 4370 (1976).
(14) D. R. Kearns, *Prog. Nucleic Acid Res. Mol. Biol.*, **18**, 91 (1976).
(15) B. R. Reid, *Nature (London)*, **262**, 424 (1976).
(16) C. R. Jones and D. R. Kearns, *Proc. Natl. Acad. Sci. U.S.A.*, **71**, 4237 (1974).
(17) K. L. Wong, Y. P. Wong, and D. R. Kearns, *Biopolymers*, **14**, 749 (1975).
(18) K. L. Wong, P. H. Bolton, and D. R. Kearns, *Biochim. Biophys. Acta*, **383**, 446 (1975).
(19) C. R. Jones, D. R. Kearns, and K. Muench, *J. Mol. Biol.*, **103**, 747 (1976).
(20) K. L. Wong, D. R. Kearns, W. Wintermeyer, and H. G. Zachau, *Biochim. Biophys. Acta*, **395**, 1 (1975).
(21) C. R. Jones and D. R. Kearns, *Biochemistry*, **14**, 2660 (1975).

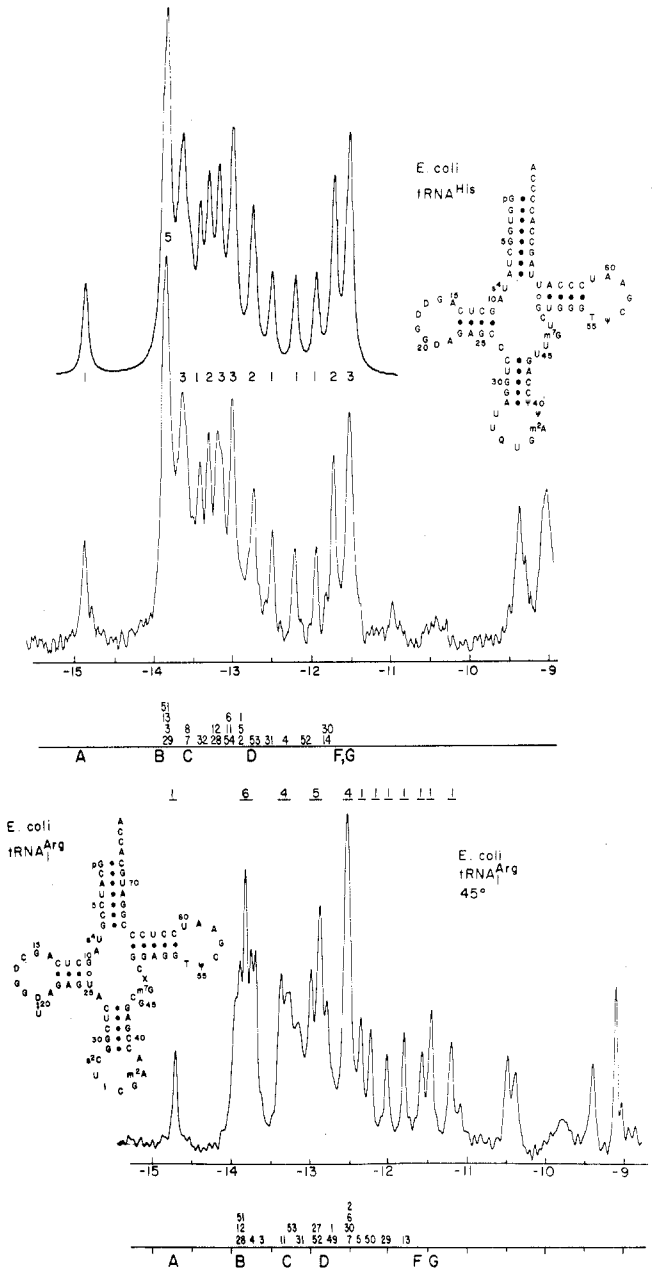

Figure 4. The low-field 360-MHz NMR spectra of *E. coli* $tRNA^{His}$ and $tRNA^{Arg}_1$. Conditions are as in Figure 1. The predicted secondary resonances and extra tertiary resonances are shown at the bottom and the computer simulation of the $tRNA^{His}$ spectrum is shown at the top.

ration methods which we used to assign secondary resonances in fragments[22] are inapplicable. Obviously the assignment of these extra peaks first requires reliably establishing which peaks are in fact the tertiary resonances. We have used three approaches to answering these questions: (a) determining which resonances are excessively sensitive to temperature changes at constant ionic strength or to magnesium ion changes at constant temperature; (b) predicting the 20 secondary resonance positions from ring-current shift values in conjunction with the known helical sequences; (c) comparison of isoaccepting tRNAs for a single amino acid and related species with minor variations in their tertiary base pairing.

We have already discussed the magnesium-dependent shifts of resonances at −13.5, −12.8, and −12.2 ppm in *E. coli* $tRNA^{Val}_1$ at physiological temperatures (see Figure 2). The fact that the rest of the spectrum remains remarkably constant argues against attributing these changes to rearrangements of secondary helices. Even better diagnostic evidence comes from temperature-dependent studies. At intermediate temperatures the least stable helices in tRNA begin to open and thus lose their low-field resonances by water exchange. When a magnesium-limited *E. coli* $tRNA^{Val}$ sample at 46 °C is raised to 54 °C discrete intensity losses are observed at −13.5, −12.8, and −12.2 ppm as well as at −14.9, −14.3, and −11.5 ppm. Observation of their line width as these resonances disappear indicates a reasonably slow exchange process and strongly suggests tertiary resonances at these positions.

An independent method of establishing which are the tertiary resonances is to attempt to predict the 20 secondary resonance positions from neighboring ring-current shifts and thus identify the extra tertiary resonances subtractively. The theoretical ring-current shift values from nearest-neighbor base pairs calculated by Giessner-Prettre and Pullman[23] were initially altered to account for the early tRNA spectra on the assumption that all observed resonances were derived from secondary cloverleaf base pairs only;[10] these values have recently been re-revised by Kearns.[14]

There are at least two serious conceptual errors in calibrating ring-current shifts by this empirical method. Firstly, the position of each neighboring base was calculated on the assumption that tRNA contains 12-fold A′ helices;[10,14] the three major secondary helices are in fact 11-fold A helices in the crystal structure.[3] Secondly, only nearest neighbor effects were considered;[10,14] the 6.8-Å-distant next-to-nearest neighbor shifts are predicted to contribute quite significant second-order effects.[24]

In our studies of many tRNAs and hairpin fragments we have obtained several spectra which cannot be rationalized by either the original or the revised method of predicting resonances. We have had much more success in treating our data according to the values of Arter and Schmidt[24] in which the first- and second-order ring-current shifts from positions calculated on 11-fold A RNA geometry are derived from the ring current of each base. We illustrate an example in the case of *E. coli* $tRNA^{Val}$ in Figure 1.

Previous studies on model RNA hairpin helices have indicated that the inherent unshifted A·U° value is to lower field than the unshifted G·C° position (A·U° should be envisaged as the theoretical chemical shift of a single isolated A·U base pair to which the upfield shifts produced by stacking neighbors will be added). In *E. coli* $tRNA^{Val}$ the summated first- and second-order shifts from above and below on base pairs 12, 29, 6, and 4 are all between 0.55 and 0.64 ppm when calculated according to the Arter and Schmidt values for 11-fold helices;[24] these are the least upfield shifted A·U base pairs in the secondary structure and are therefore expected at the low-field end of the spectrum. In Figure 1 the lowest field group of four resonances observed experimentally occurs between −13.8 and −13.7 ppm.

(22) D. R. Lightfoot, K. L. Wong, D. R. Kearns, B. R. Reid, and R. G. Shulman, *J. Mol. Biol.*, **78**, 71 (1973).

(23) C. Giessner-Prettre and B. Pullman, *J. Theor. Biol.*, **27**, 87 (1970).

(24) D. B. Arter and P. G. Schmidt, *Nucleic Acids Res.*, **3**, 1437 (1976).

This leads to a value of −14.35 ppm for A·U° which differs from previous values which were chosen to rationalize mis-assigned resonances;[10,14,16,19-21] similar treatment of G·C resonances in tRNA spectra and simpler hairpin helix spectra leads to a value close to −13.4 ppm for G·C°.

This analysis has been extended to cover over 200 individual base pairs in several tRNAs, and this has increased our confidence in utilizing the Arter and Schmidt ring-current shift values.[24] Furthermore, this method also successfully predicts the resonances observed in our simpler spectra of hairpin fragments. Thus in Figure 1 there are five secondary resonances predicted between −13.4 and −13.8 ppm, and the observed extra resonance at −13.4 ppm is denoted C since peaks A and B at −14.9 and −14.3 ppm are also not predicted from secondary structure. At the bottom of Figure 1 the predicted secondary resonances are denoted by their base-pair number and the unpredicted extra resonances are designated A, B, C, D, E, F, G.

Similar treatment of the spectra of *E. coli* $tRNA^{Met}_{m}$ and $tRNA^{Gly}_{3}$ (and several other tRNAs including yeast $tRNA^{Phe}$) also lead to extra resonances with similar chemical shifts, as shown in Figure 3. It might at first appear puzzling why different tRNAs with different sequences should have their tertiary resonances at similar chemical shifts. However, the tertiary interactions involve bonding to, and extension of, the h_2U helix.[3] For this reason we chose a series of class-1 tRNAs with identical h_2U helices in the hope of maintaining a similar environment for the tertiary interactions. We noted earlier that under limiting magnesium conditions at intermediate temperatures we observed selective destabilization of base-pair resonances at precisely the positions where the extra tertiary resonances are predicted by subtractive methods.

Tertiary Assignments

We, and others, have assigned the resonance at −14.8 ± 0.1 ppm to the s^4U8–A14 tertiary base pair by dethiolating s^4U8 to U8; this causes the −14.9-ppm resonance to move to −14.2 ppm.[18,25] Further corroboration for this assignment can be seen in the spectrum of a $tRNA^{Gly}_{3}$ sample in Figure 3 which was found naturally to contain 30% s^4U8 and 70% U8; 30% of the 8–14 resonance is at −14.75 ppm and the other 70% is at −14.25 ppm.

Tertiary resonance B is at −14.3 ppm in *E. coli* $tRNA^{Val}$; this is the theoretically unshifted position of a normal Watson–Crick A·U base pair and suggests something abnormal about either the base pair of its environment. Apart from the 8–14 interaction there is only one other A·U-type tertiary interaction, and it is T54–A58.[3] Since G·C base pairs cannot resonate at such low fields we deductively assigned tertiary resonance B to T54–A58 and subsequently obtained several pieces of evidence to support this assignment.

As we have discussed, the four lowest field secondary A·U resonances are within 0.1 ppm of each other, and hence the lone single proton at −14.3 ppm cannot be one of them. Secondly, the isolated rT stem hairpin of $tRNA^{Val}$ is not expected to contain any resonances lower than −13.2 ppm; however we have observed the T54–A58 resonance as an extra peak at −14.3 ppm in the spectrum of this fragment. Thirdly, the position of tertiary resonance B in a series of tRNAs is sensitive to the sequence surrounding T54 and A58. Hence in yeast $tRNA^{Phe}$ and *E. coli* $tRNA^{Val}$ the T54–A58 resonance is at −14.3 ppm; Kearns and colleagues have either not acknowledged this interaction[20,21] or mis-assigned the T54–A58 interaction in yeast $tRNA^{Phe}$ and in *E. coli* $tRNA^{Val}$ at −13.8 ppm.[13,14] The T54–A58 interaction is an abnormal reversed Hoogsteen base pair.[3] Robillard et al.[26] have discussed the extra downfield shift expected from such atypical hydrogen bonding.

The remaining five tertiary interactions all involve guanosine ring NH hydrogen bonds and are G15–C48, G19–C56, m^7G46–G22, G26–A44, and possibly G18–ψ55.[3] *E. coli* $tRNA^{Val}_{1}$, $tRNA^{Met}_{m}$, $tRNA^{Gly}_{3}$ all contain the Pu26–Pu44 interaction (either G26–A44 or A26–G44) seen crystallographically in yeast $tRNA^{Phe}$ and all contain the seven tertiary low-field resonances A, B, C, D, E, F, G. However, this Pu–Pu ring NH interaction is not possible in $tRNA^{His}$ or $tRNA^{Arg}$ (see Figure 4). In $tRNA^{Arg}$ the seven resonances observed between −11.9 and −12.7 ppm are all predicted by secondary base pairs 29, 50, 5, 2, 6, 30, 7, and hence there is no extra resonance E, although the tertiary resonances A, B, C, D, F, G are still observed. The loss of this low-field tertiary resonance presumably reflects the fact that $tRNA^{Arg}_{1}$ contains A26 and C44, neither of which contain a ring NH proton. In $tRNA^{His}$ (in which the corresponding positions are occupied by C and U residues, respectively) the tertiary resonance E is also lost. Furthermore, in *E. coli* $tRNA^{Lys}$, which contains A26 and U44,[27] the 26–44 resonance reappears at lower field, presumably reflecting an A·U base pair between these positions. Hence this type of comparative spectroscopy indicates that the tertiary resonance at ∼−12.3 ppm is derived from Pu26–Pu44 in species where purines occupy these positions. The Pu26–Pu44 resonance is usually found between −12.1 and −12.5 ppm since its immediate environment (C·G at the top of the anticodon helix and G-C10 at the base of the h_2U helix) is constant in the species we have chosen; the slight variation we observe is presumably the result of 0.1–0.2 ppm changes in second-order shifts.

Similar comparative studies on *E. coli* $tRNA^{Gly}_{3}$ $tRNA^{Gly}_{2}$ (no m^7G46), and $tRNA^{Gly}_{1}$ (no m^7G46 or 15–48 interaction) indicate that either peak F or peak G at ∼−11.6 ppm is the 15–48 tertiary interaction and that resonance C is the m^7G46–G22 tertiary interaction. The m^7G46–G22 resonance was independently assigned at −13.4 ppm by chemical removal of m^7G46 from several tRNAs. The unexpectedly low-field position of this G N1H resonance is the result of a large deshielding effect on all protons in m^7G by delocalization of the positive charge at N-7. The occurrence of the G15–C48 resonance at the high-field end of the spectrum probably reflects the fact that this is a reverse Watson–Crick base pair in which the G15 ring NH bonds to an exocyclic carbonyl oxygen;[3] such bonding is less deshielding than normal Watson–Crick bonding.[4] Hence we have established that A is 8–14, B is 54–58,

(25) B. R. Reid, N. S. Ribeiro, G. Gould, G. Robillard, C. W. Hilbers, and R. G. Shulman, *Proc. Natl. Acad. Sci. U.S.A.*, **72**, 2049 (1975).

(26) G. T. Robillard, C. E. Tarr, F. Vosman, and H. J. C. Berendsen, *Nature (London)*, **262**, 363 (1976).

(27) K. Chakraburtty, A. Steinschneider, R. V. Case, and A. H. Mehler, *Nucleic Acids Res.*, **2**, 2069 (1975).

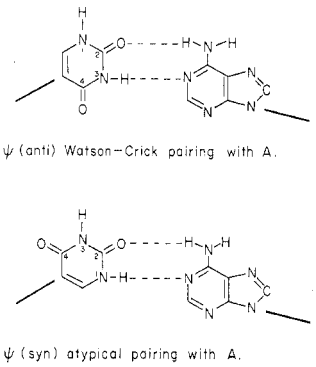

Figure 5. Normal (anti) and atypical (syn) base pairing of pseudouridine with adenosine involving rotation of the glycosidic bond.

C is 46–22, E is 26–44, and F or G is 15–48.

We have not yet chemically or biochemically assigned G19–C56 which is constant in all tRNAs. The only remaining tertiary positions for it are −12.8 ppm (D) or −11.5 ppm. The G19–C56 interaction is the only standard Watson–Crick tertiary base pair[3] and hence will have the normal G·C° starting position at −13.45 ppm. In the crystal structure this base pair is stacked on only one side with G57.[3] It is difficult to envisage an upfield shift of more than 0.7 ppm on this resonance, and hence peak D at ∼−12.8 ppm is the only reasonable assignment for the G19–C56 tertiary base pair. This leaves one remaining resonance at ca. −11.5 ppm (F or G). Its identity is not obvious, and it may be derived from G18–ψ55. However our recent data on hairpin fragments suggest that it may well be the U–NH hydrogen bond of the G·U pair often found in tRNA.

A•ψ Base Pairs and Regulatory tRNAs

Several tRNAs contain an A·ψ base pair at the base of their anticodon helix which is apparently important in regulation since mutant bacterial strains with A·U substitution for A·ψ in this position pleiotropically produce high derepressed levels of the biosynthetic enzymes for the amino acid attached to that tRNA.[28] We are interested in studying the structural basis for the regulatory capacity of these A·ψ-containing tRNAs, and in the course of studying several such species, as well as helical hairpin fragments containing A·ψ base pairs,[22] we have noted an anomaly in the A·ψ low-field resonance. The inherent starting A·U° position is −14.35 ppm and the downfield shift on U N.3–H by the in-plane ring current of A should be the same in A·U pairs and A·ψ pairs.

However, our observed A·ψ resonances cannot be accounted for using a −14.35-ppm starting position, and we have been forced to use an inherent A·ψ° chemical shift of −13.7 ± 0.2 ppm to rationalize our tRNA and fragment spectra. While wondering about this anomaly we realized that ψ, unlike U, has two ring NH protons available for hydrogen bonding, and these are not chemically equivalent. In ψ the extra N1H resonates almost 0.5 ppm to higher field than the uridine N3H and theoretically pseudouridine could base pair with adenine either via a normal N3H hydrogen bond in the anti conformation or via an abnormal N1H hydrogen bond in the syn conformation as shown in Figure 5.

(28) R. Cortese, R. Landsberg, R. A. vonder Haar, H. E. Umbarger, and B. N. Ames, *Proc. Natl. Acad. Sci. U.S.A.*, 71, 1857 (1974).

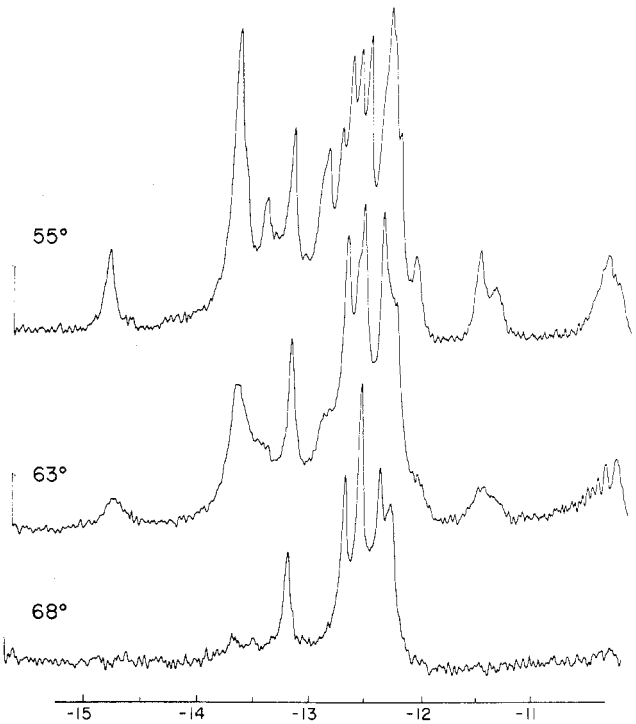

Figure 6. The NMR spectra of intermediate states in the thermal unfolding of *E. coli* $tRNA^{Phe}$. The original spectrum at 40 °C contained 27 base-pair resonances; the 68 °C spectrum contains six sharp resonances and one broad resonance (at −13.75 ppm) from the seven base-pair acceptor stem. The extremely broadened resonance at −13.75 ppm is derived from the terminal base-pair A·U7.

Only the latter pairing would explain the anomalous upfield position of A·ψ resonances compared to A·U resonances, and hence we propose that the regulatory A·ψ base pair involves abnormal hydrogen bonding in the syn conformation via the N1 proton.

The N3H and oxygen-4 in the major groove might perhaps stabilize a conformation of tRNA which is essential to genetic regulation. We have suggested that ψ39 in yeast $tRNA^{Phe}$ might be rotated about the glycosidic bond into the syn conformer. Quigley and Rich[29] have examined the x-ray structure in this light; they report that further refinement is necessary to unambiguously answer this question in the crystal structure.

The Thermal Unfolding Sequence of tRNAs

When a given helix begins to unfold as a result of heating, the ring NH protons exchange rapidly with H_2O and are lost from the low-field spectrum. This can occur via broadening if the helix lifetime is reduced below 1–2 ms as one approaches the t_m, or without broadening if the helix lifetime remains longer than ca. 10 ms at the t_m. An example is shown in Figure 6. In *E. coli* $tRNA^{Phe}$ the tertiary base pairs are destabilized first followed closely by the rT helix and h_2U helix. The anticodon helix is the second last to "melt", and finally the acceptor helix melts. At 68 °C only the acceptor stem resonances from the six G·C pairs are left plus a broadened resonance from A·U7 at −13.7 ppm.

Tertiary Base Pairs in Class-3 tRNAs

Although most tRNAs contain a five-nucleotide variable loop (class-1 D4V5), some tRNA species

(29) G. J. Quigley and A. Rich, *Science*, 194, 796 (1976).

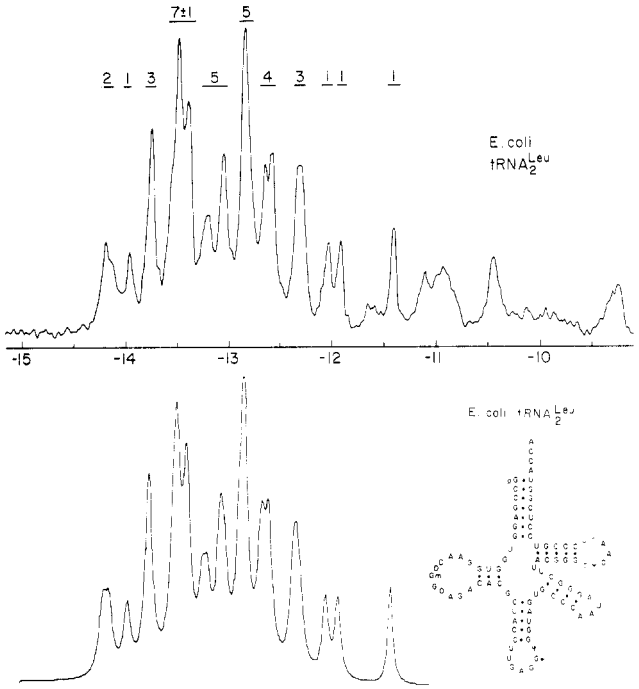

Figure 7. The low-field 360-MHz NMR spectrum of *E. coli* $tRNA^{Leu}_2$ at 35 °C. Conditions are as in Figure 1. The intensities are indicated above each peak, and the computer simulation is shown below the experimental spectrum.

contain a large, internally base-paired, variable loop containing up to 21 nucleotides (class-3 D3VN species where N is 13–21 residues). We have examined the low-field spectra of several class 3 D3VN tRNAs, and *E. coli* $tRNA^{Leu}_2$ is shown in Figure 7 as an example. The spectrum contains several resolved peaks, and the total intensity between −11 and −15 ppm integrates to 33 ± 1 protons, reflecting ca. 33 long-lived base pairs. The secondary structure contains only 23 base pairs, and we thus observe ~10 extra resonances derived from tertiary base pairing. We observe 33-proton spectra containing approximately 10 tertiary base-pair resonances in all four *E. coli* leucine tRNAs and two tyrosine tRNAs and conclude that class-3 D3VN tRNAs contain even more extensive tertiary base pairing in solution than class-1 tRNAs. The opposite conclusion has been made in a study of leucine tRNA species from yeast by Kearns and co-workers.[14,30–32] They report only ~22 protons in the low-field spectra of the class-3 leucine tRNA species they studied. Their errors result from the use of wrong internal and external intensity standards.[30]

Summary

We have shown the usefulness of high-resolution NMR in monitoring the base-pairing and three-dimensional folding of tRNA in solution. Modern technical innovations permit excellent spectra to be obtained in 10 min on a few milligrams of sample. Reliable assignment of the spectra now permits structural perturbations to be accurately interpreted, although several premature attempts have already been made on spectra which were assumed to contain no tertiary resonances from three-dimensional folding.[14,16,17,20,21] We have restricted ourselves to the low-field NMR spectrum of tRNA. However, useful corroborative structural data can also be obtained from the methyl and methylene resonances in the 0 to −4 ppm spectral window.[33,34]

We are extremely indebted to Susan Ribeiro and Lillian McCollum in this laboratory for superb assistance in purifying several tRNA species to homogeneity. Thanks are also due to Dr. J. Abbate of this laboratory and Dr. G. T. Robillard of the University of Groningen for helpful discussions and the use of the Groningen 360-MHz spectrometer (supported by the Netherlands Z.W.O) during the early stages of this work. We gratefully acknowledge the use of the Stanford Magnetic Resonance Laboratory Bruker HXS 360 spectrometer (supported by NSF Grant GR23633 and by NIH Grant RR00711) and especially Dr. W. W. Conover and Dr. S. L. Patt for advice in running correlation spectra. This work was supported by grants from the American Cancer Society (NP-191), the National Science Foundation (PCM73-01675), and the National Cancer Institute, DHEW (CA11697).

(30) D. R. Kearns, Y. P. Wong, S. H. Chang, and E. Hawkins, *Biochemistry*, **13**, 4736 (1974).
(31) D. R. Kearns, P. Wong, E. Hawkins, and S. H. Chang, *Nature (London)*, **247**, 541 (1974).
(32) B. F. Rordorf, D. R. Kearns, E. Hawkins, and S. H. Chang, *Biopolymers*, **15**, 325 (1976).
(33) L. S. Kan, P. O. P. Ts'o, F. v. d. Haar, M. Sprinzl, and F. Cramer, *Biochem. Biophys. Res. Commun.*, **59**, 22 (1974).
(34) R. V. Kastrup and P. G. Schmidt, *Biochemistry*, **14**, 3612 (1975).